Research Article | Vol. 31, No. 12 / 5 Jun 2023 / Optics Express 19146
Optics EXPRESS

Free-electron laser temporal diagnostic beamline FL21 at FLASH

ROSEN IVANOV,[1,2] MAHDI M. BIDHENDI,[1,*] IVETTE J. BERMÚDEZ MACIAS,[1,2] MACIEJ BRACHMANSKI,[1] SVEA KREIS,[1] SUSANNE BONFIGT,[1] MARKUS DEGENHARDT,[1] MARIE-KRISTIN CZWALINNA,[1] MIKHAIL PERGAMENT,[3] MARTIN KELLERT,[3] FRANZ X. KÄRTNER,[3,4] AND STEFAN DÜSTERER[1]

[1]*Deutsches Elektronen-Synchrotron DESY, Notkestr. 85, 22607 Hamburg, Germany*
[2]*Currently with the European XFEL GmbH, Holzkoppel 4, D-22869 Schenefeld, Germany*
[3]*Center for Free-Electron Laser Science CFEL, Deutsches Elektronen-Synchrotron DESY, Notkestr. 85, 22607 Hamburg, Germany*
[4]*Department of Physics, Universität Hamburg, Jungiusstr. 9, 20355 Hamburg, Germany*
[*]*mahdi.mohammadi-bidhendi@desy.de*

Abstract: A beamline for temporal diagnostics of extreme ultraviolet (XUV) femtosecond pulses at the free-electron laser in Hamburg (FLASH) at DESY was designed, built and put into operation. The intense ultra-short XUV pulses of FLASH fluctuate from pulse to pulse due to the underlying FEL operating principle and demand single-shot diagnostics. To cope with this, the new beamline is equipped with a terahertz field-driven streaking setup that enables the determination of single pulse duration and arrival time. The parameters of the beamline and the diagnostic setup as well as some first experimental results will be presented. In addition, concepts for parasitic operation are investigated.

1. Introduction

Free-electron lasers (FELs) working in the extreme ultraviolet (XUV) and X-ray region deliver photon pulses with a duration in the femtosecond (fs) range with unrivaled intensity [1–6]. The majority of X-ray FELs operate in the self-amplified spontaneous emission (SASE) regime, meaning that each pulse is characterized by a unique combination of pulse energy, XUV spectrum, arrival time and pulse duration. The necessity to know the duration and temporal profile of each individual pulse stimulated the development of different methods that are suitable for single-shot temporal characterization. A few years ago, a study was carried out on different temporal diagnostic techniques [7], which led to the decision that field-driven terahertz (THz) streaking fulfills most of the requirements for FLASH compared to other techniques. The THz field-driven streaking technique [8,9] has the potential to deliver single-shot pulse duration information essentially wavelength-independent from XUV to X-rays with a large dynamic range in pulse duration and FEL pulse energy. It can be operated with repetition rates up to several hundred kHz [10] (potentially even MHz) and absorbs only a tiny fraction of the incident photons and can thus be in principle transparent to the XUV beam. In order to investigate the capabilities of THz streaking as well as its limits in more detail and start to establish the technique as a standard diagnostic tool, a dedicated beamline (FL21) was designed, built and commissioned to host permanently a THz streaking setup. Parts of the THz streaking setup described here have already been used in dedicated diagnostic beamlines at FLASH1, exploring the potentials of the technique [11–13]. However, a permanent setup including an own optical laser system generating

#492228 https://doi.org/10.1364/OE.492228
Journal © 2023 Received 11 Apr 2023; revised 8 May 2023; accepted 9 May 2023; published 23 May 2023

Optics EXPRESS

the THz pulses is mandatory to guarantee a stable operation. To allow a parasitic measurement of the pulse duration, a concept has been implemented to extract a small fraction of the FEL beam for the diagnostic setup while the remaining part can still be used by a different experiment.

2. Beamline FL21 at FLASH2

2.1. Concept

To provide a constant THz streaking field and thus reliable data, the FEL beam diameter in the THz streaking setup has to be significantly smaller than the THz focal diameter. In order to achieve the highest streaking fields for good temporal resolution, the THz beam is almost diffraction limited focused to a beam diameter of around 1 mm full width at half maximum (FWHM), which is much smaller than the unfocused FLASH beam (3-10 mm FWHM) in the experimental hall. Thus, it is not possible to install our setup directly in the main beamline without focusing the FEL beam. Our approach is to extract a part of the FEL beam and focus it in order to provide the conditions for a dedicated pulse duration diagnostic. Since there is no standard way to realize a nondestructive XUV beam splitter, we chose a geometry using a "cutting mirror" (moving up-down) that reflects a fraction of the beam to the THz streaking setup while the remaining part of the XUV beam propagates along the beamline similar to concepts used in XUV split and delay units [14–17]. As will be shown in section 4, the temporal properties of the SASE XUV pulse can still be reliably measured, even if only a fraction of the beam is used for the diagnostic.

2.2. Beamline layout

We designed and built the beamline FL21 (scheme in Fig. 1 and details in Fig. 2) consisting of a flat cutting mirror (CM) "splitting" the FEL beam; focusing (toroidal with 1.5m focal distance) mirror (FM); Laser-based THz source, THz streaking setup (TSS) in a laser safety hutch (LSH) and a direct beamline branch for the remaining FEL beam at which additional diagnostics (spectrometer, XUV pulse energy measurement) can be installed for calibration measurements or further developments. Figure 2 presents the detailed drawing of the beamline starting with the Cutting Mirror (CM) mounted in a UHV 160 CF cube on a three-axis motorized manipulator in a 40 CF flange together with an in-vacuum manual two-angle kinematic mount (for pre-alignment). The CM and its mount are designed to cut the XUV beam precisely without parasitic reflections while avoiding unnecessary losses (inset in Fig. 2). For a well-defined cutting edge and to avoid

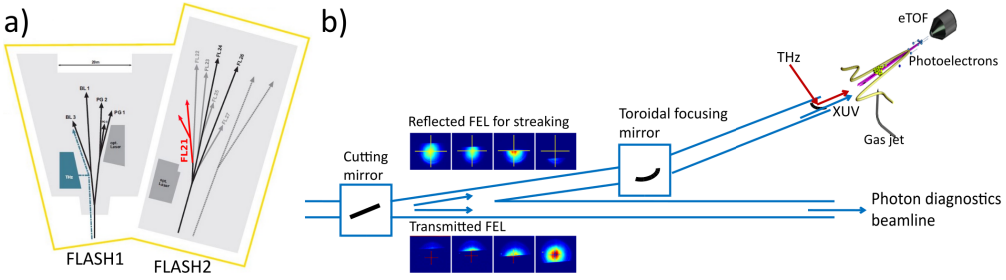

Fig. 1. a) Overview layout of the FLASH1 and FLASH2 experimental halls. The FL21 beamline is indicated in red. b) Top view of the FL21 beamline at FLASH2. The beamline consists of two branches that can share the FEL beam by introducing a cutting mirror. The cutting mirror moves up and down (perpendicular to the shown top view) so that part of the beam can be reflected to the THz streaking setup (upper branch) while the remaining part of the FEL beam propagates straight to an open port beamline dedicated to general photon diagnostic measurements.

Optics EXPRESS

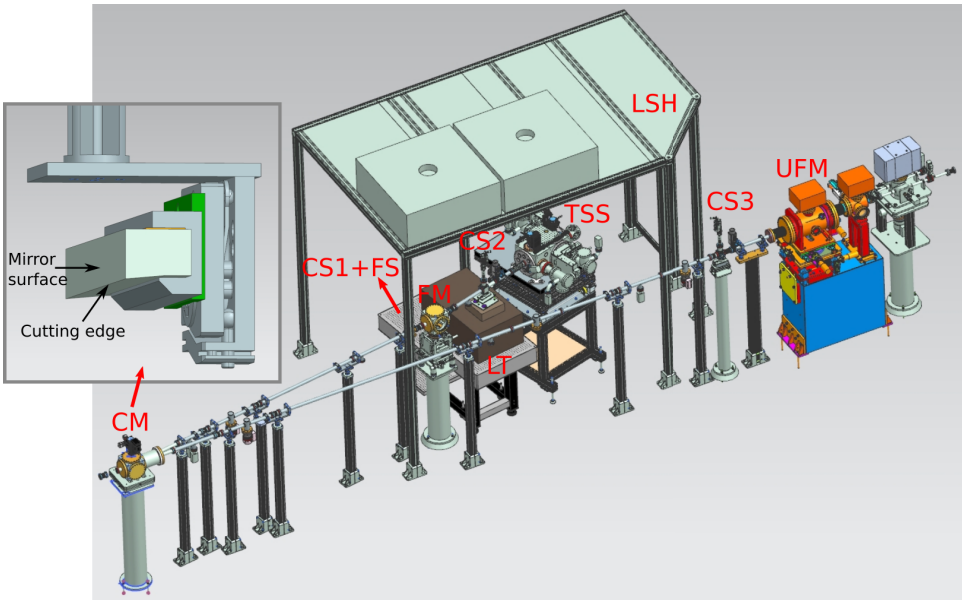

Fig. 2. 3D drawing of the FL21 beamline consisting of a flat cutting mirror (CM), focusing mirror (FM), a laser safety hutch (LSH) for the THz streaking setup (TSS) including a laser-based THz source and a direct beamline branch including a focusing mirror for the remaining FEL beam. The inset shows a drawing of the cutting mirror, showing the specially designed cutting edge and the mirror surface.

reflections on the bottom surface, the lower edge is cut at an angle of 85° thus the mirror can be coated with gold (Au) almost up to the edge (< 0.1 mm). A special mechanical mount had been designed only partially enclosing the mirror such that the lower part remains free to not block the transmitted beam. We did not observe any deformation of the mirror due to the reduced support. Moving the CM vertically we can reflect a fraction of the FEL beam into the THz streaking hutch while the unaffected fraction of the FEL beam propagates on a straight path (outside LSH) and reaches the experimental chamber. The part of the beam that was reflected from CM reaches the focusing mirror (FM) installed in a UHV 160 CF cube mounted on a motorized support that can provide three translational axes and three angle degrees of freedom for alignment. The cutting as well as the focusing mirror are coated with gold (Au) to cover the wavelength range of ~ 7 nm to ~ 50 nm. Both mirrors have a size of 150 x 15 mm, leading to a horizontal "footprint" (clear aperture) of around 10.7 mm at a grazing incidence angle of 4°. The toroidal mirror has a focal distance of 1.5 m and provides a focal spot size of 100 to 200 μm FWHM depending on the FEL parameters. It was verified that the focal spot size does not significantly change for different fractions of the beam reflected by the cutting mirror. The focus position is aligned to be in the interaction point of the THz Streaking setup (TSS). In front (upstream) of the FM chamber a one-axis motorized CF40 manipulator was installed containing a Ce:YAG crystal ($20\times20\times0.2$ mm) that is monitored by a CCD camera to observe the FEL beam shape (CS1+FS). Additionally, on this manipulator there are four thin metal filters of different materials installed to adjust the pulse energy entering the TSS independently of the straight "uncut" FEL beam. A second CCD camera and Ce:YAG crystal screen (CS2) on a pneumatic mover are installed between FM and TSS. A similar setup CS3 (Ce:YAG screen plus CCD camera) has been installed near the end of the straight branch outside the LSH. Recently, at that position, a focusing mirror (UFM) chamber (previously located at the decommissioned beamline BL2 at FLASH1 [18])

Optics EXPRESS

was installed providing a ~ 20 μm focus (or unfocused beam) dedicated to photon diagnostics measurements.

The initial alignment of all FL21 beamline elements was done using the beamline pilot laser which was aligned with respect to the nominal beam axis of the FEL. With that source and CS1, CS2, CS3 plus an additional TSS interaction point spatial observing system (screen and camera with a variable (up to x12) magnification lens), the beamline elements were aligned and reference beam positions were set. For the FEL operation we use the beamline mirrors located in the FLASH2 accelerator tunnel to align the FEL to our reference positions.

3. Pulse duration diagnostic setup

We first describe the initial setup that was used in several previous measurement campaigns [11–13,19]. In the second part, a recently upgraded version with more electron time-of-flight (eTOF) spectrometers with improved handling is presented.

3.1. Initial setup

The initial pulse duration diagnostic setup consists of an IR laser system, a setup to generate the THz single-cycle pulses and an interaction chamber equipped with an electron spectrometer. The IR laser system, as well as the THz streaking setup (TSS), are placed to confine the laser radiation in a dedicated laser safety hutch (LSH) equipped with a laser interlock system. The actual laser system consists of a commercial oscillator (Onefive ORIGAMI, 1030 nm, 8 nm bandwidth) which is optically synchronized to the FLASH main laser oscillator (MLO) with a sub-10 fs rms jitter [20], and an in-house built regenerative amplifier. The Yb:KYW regenerative amplifier was implemented using a dual-crystal approach to distribute the thermal load and balance the thermal lens in the gain media. The amplifier's dual-crystal cavity enables stable operation over a wide pumping power range and provides a stable output at repetition rates of up to 1000 Hz. Stretching of the seed pulse and compression of the amplified output is accomplished using chirped-volume-Bragg-gratings in the amplifier unit. That ensures the pointing stability of the amplifier's output and makes the design robust and reliable (1030 nm, 3 nm bandwidth 3.5 mJ, 1 ps, 10 Hz) [21]. The single-cycle THz generation based on optical rectification in $LiNbO_3$ utilizing a tilted pulse front (similar to Ref. [11]) was built on the second level of our optical laser table (LT). Here, a diffractive grating with 1500 grooves per mm disperses the IR beam which is imaged by a 4f telescope (focal lengths of 200 mm and 125 mm) onto the $LiNbO_3$ crystal prism. This scheme produces a tilted pulse front satisfying the phase-matching condition for optical rectification and thus efficient THz production with ~ 0.1% THz efficiency [22]. The THz setup is located on a separate small optical breadboard which is connected to the LT and placed near the streaking chamber to minimize the THz optical path in air (~ 55 cm) until it enters the vacuum chamber of the TSS. The THz transport consists of two flat and two 90° off-axis parabolic mirrors (PM). PM1 collimates the THz with a reflective focal length of 6" (152.4mm) and PM2 focuses the THz into the interaction point. PM2 (with focal length of 4" (101.6 mm)) has a 3 mm hole in the middle allowing the FEL beam to overlap collinearly with the THz focus. All THz transport optics are gold coated and only PM2 is located in vacuum. To transmit the THz beam into the TSS a vacuum window consisting of Zeonex 480R polymer is used. The overall THz transport has a clear aperture > 50 mm and a transmission of ~ 90%.

The single-cycle THz pulse has a linear slope of ~ 500 fs (an example shown in Fig. 4), centered at 0.7 THz with a pulse energy of ~ 3 – 4 µJ. The THz generation setup was optimized to produce a high THz field with a steep linear slope (see Fig. 4 a) and d)) in order to increase the streaking resolution for measuring relatively short (<50 fs) SASE FEL pulses. Thus, the THz beam was tightly focused to horizontally 1.2 ± 0.1 mm and vertically 1.5 ± 0.1 mm FWHM (see Fig. 3 c)) observed by a pyroelectric camera (Spiricon Pyrocam III), leading to a field strength of

Optics EXPRESS

up to 150 kV/cm. This focusing geometry leads to a Gouy phase broadening [12,23] of about 15 fs (FWHM) which has to be taken into account for the data analysis.

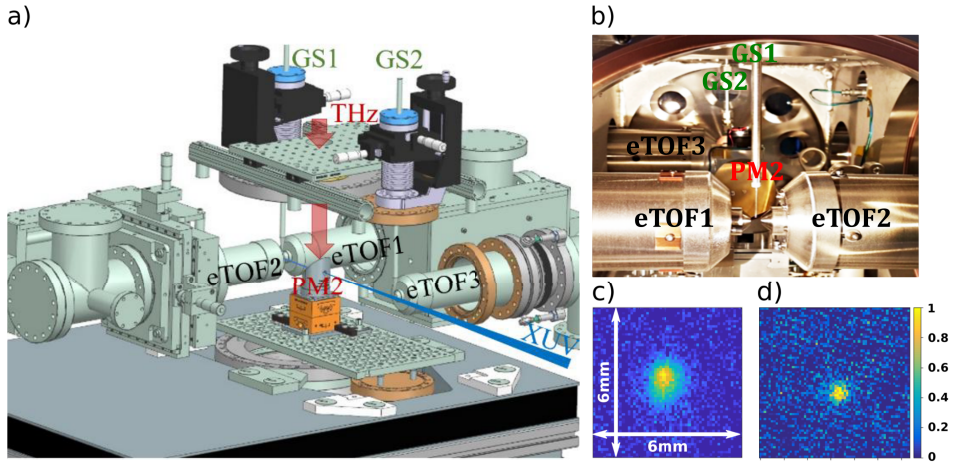

Fig. 3. a) Upgraded THz streaking setup consisting of three eTOFs (vacuum chamber is not visible). b) Picture inside the vacuum chamber showing three eTOFs and two gas sources. c) THz foci measured with a pyroelectric camera. left: initial setup with 1.2 mm x 1.5 mm focus; right: Upgraded setup with 0.9 mm x 0.9 mm focus.

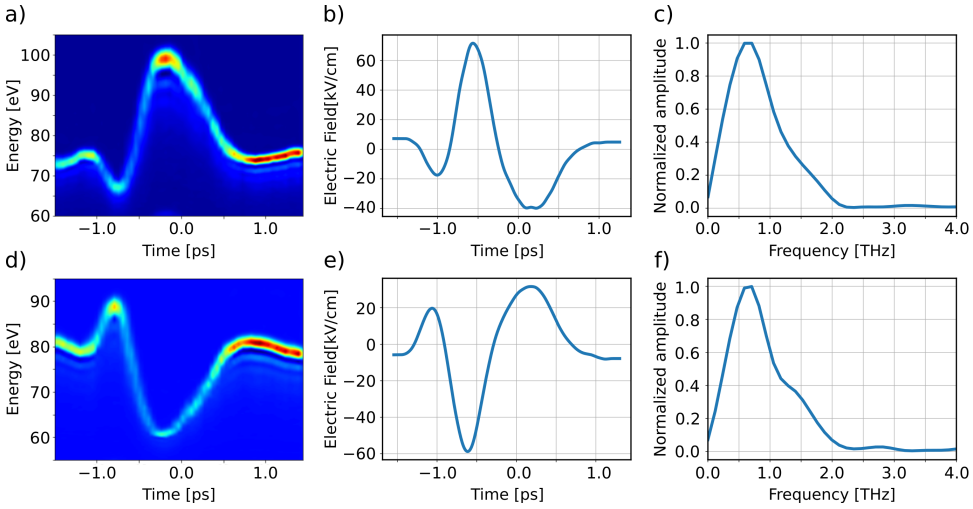

Fig. 4. THz Streaking trace (delay scan) for neon 2p photoelectrons ionized by 13 nm XUV pulses and measured simultaneously by a) eTOF1 and d) eTOF2. The streaking trace is proportional to the vector potential of the THz pulse. The THz electric field was calculated by differentiating the vector potential measured by b) eTOF1 and e) eTOF2. c) and f) show the spectral distribution of the electric field calculated by a Fourier transform for eTOF1 and eTOF2 respectively.

The THz streaking setup (TSS) hosts besides various diagnostics and the gas supply, the THz focusing and the eTOF. The FEL and the THz beam (both with horizontal linear polarization) were overlapped spatially and temporally in the acceptance volume of (~ 0.5 mm^3) of the eTOF (Kaesdorf ETF11) which we define as the interaction point of the TSS. More details on the

Optics EXPRESS

overlap procedure can be found in Ref. [11]. FLASH typically operates in a burst mode, resulting in several hundred XUV pulses with a separation of up to 1 μs with a burst repetition rate of 10 Hz [1]. The THz source on the other hand operates at 10 Hz repetition rate and thus we can only "streak" one FEL pulse in the burst. Using the trigger and synchronization system one can jump easily to different pulses in the FEL burst to successively measure the properties of the pulses along the burst. The advantage of the burst structure is that with the same eTOF one can record for each 10 Hz measurement the "streaked" XUV pulse and "unstreaked" reference pulses that were not altered by the THz field. These "reference pulses" are needed for the analysis, since essentially the pulse duration is encoded in the difference between the streaked and the unstreaked (reference) photoelectron line width (for theoretical explanation see e.g. [8,9,12,23]). Using a second FEL pulse produced only 1 μs later than the streaked one as the reference is a good approach and is used for standard analysis. For pulse durations > 50 fs the widths of the streaked spectra is sufficiently broader than the unstreaked (reference) spectrum and thus one can utilize a different FEL pulse as the reference. The pulse to pulse fluctuation of the unstreaked spectra are sufficiently small. For short pulses < 50 fs the broadening of the streaked pulses is rather small and the reference should be taken from the *same* SASE FEL pulse that is streaked. To be able to acquire such a reference spectrum an additional eTOF located upstream the THz incoupling is needed.

3.2. Upgraded setup

After successful measurements with a streaking setup containing one eTOF, a new chamber containing three eTOFs was build to widen the experimental capabilities. Having two eTOFs in the polarization plane of the THz, but in opposing directions, allows to record simultaneously the streaked photo electron spectra created by the XUV pulse interacting with the same THz field but with opposite sign. This option allows a determination of the resolution of the arrival time measurements (see below) and enables us to characterize statistical errors in the pulse duration measurements as well as the measurement of the single shot chirp of the XUV pulses like discussed in Refs. [8,23].

Recently, such an upgraded THz streaking setup was installed at FL21. The new chamber hosts three eTOF (Fig. 3) and a modified THz incoupling. The new chamber ($310 \times 310 \times 510$ cm) was manufactured from nonmagnetic stainless steel using six 250 CF flanges and additional four 100 CF flanges on its walls. This allows us to mount three eTOFs (side walls), two noble gas sources (top), a THz window (top), a 1000 l/s turbo pump (bottom), several viewports and additional elements. The THz source remained the same, while the THz transport was adapted to the new boundary conditions. The THz is now coupled into the TSS from the top. Essentially the collimating parabola PM1 was changed to a (larger) reflected focal length of 9" (228.6 mm) with 3" clear aperture, leading to a smaller THz focal spot of 0.9±0.1 mm FWHM close to the diffraction limit (Fig. 3). The small focus however increases the Gouy phase induced broadening [12,23] to about 20-25 fs (FWHM), limiting the ability to measure short pulses below 30 fs (FWHM).

Another upgrade enables the remote control of the THz focusing parabola PM2 in the vacuum. The parabola is mounted on top of two motorized goniometers with piezo motors having the center of rotation (± 2.5°) at the position of the hole (for the FEL beam) in the reflective surface (Fig. 3). eTOF1 and eTOF2 are mounted on three-axis UHV 100CF manipulators which enable the precise alignment of the eTOFs to the XUV-THz interaction point. eTOF3 is installed upstream of the interaction region in front of the THz focusing parabola on an adjustable bellow (port aligner). The eTOFs (Kaesdorf ETF11) are differentially pumped by a 300 l/s turbo pump. The gas sources (GS1 and GS2 on Fig. 3) are also supported by three-axis UHV 40CF manipulators and each of them has a motorized gas valve to adjust the gas flow remotely and independently of each other. Typically, a chamber pressure of $1 - 9 \times 10^{-7}$ mbars (for neon) is used for the actual

Optics EXPRESS

measurements. When the gas valves are closed, the pressure of the vacuum chamber is in the 10^{-9} mbar range. The chamber pressure and the FEL pulse energy in the interaction region are adjusted such that enough electrons are created in the acceptance volume of the eTOF to get a sufficiently well-defined eTOF spectrum without leading to space charge effects (for more details see Ref. [12]). Figure 4 a) and d) present "up" and "down" streaked THz delay scans collected with eTOF1 and eTOF2, so-called streaking traces, which are proportional to the THz vector potential. The measurement shows the energy of Ne 2p photoelectrons in eV as a function of the relative delay between the THz and the FEL pulse in ps.

In summary, the upgraded setup allows us to improve and quantify single-shot temporal resolution in the arrival time and pulse duration measurements as well as the evaluation of single-shot chirp measurements. However, since these upgrades are rather recent, the quantification of the improvements that can be gained by using data from the three eTOFs is still explored and will be reported in future publications.

4. Experimental results

4.1. Testing a parasitic measurement scheme

For a standard THz streaking measurement, it is sufficient to reflect and focus only about 1 μJ of the FEL pulse (typically a small fraction of the FEL pulse energy) to the THz streaking setup. This pulse energy allows to determine the pulse duration with typically ± 20% accuracy and the arrival time with few fs accuracy [11,12]. More pulse energy would lead to undesired space charge effects. Thus, the scheme to only use a fraction of the FEL beam (reflected by the cutting mirror introduced above) seems to be applicable for future parasitic operations. It is however a rather complex task to ensure theoretically that the temporal properties of the SASE pulses are comparable throughout the entire beam profile. Most of all if there are more higher-order spatial modes present as is typically the case at FLASH. Thus, we performed several test measurements using different "splitting" ratios to investigate the evolution of the measured pulse duration as a function of the cutting fraction to tackle the problem from the experimental side. For several measurement campaigns we collected experimental data reflecting different fractions of the FEL beam to the THz streaking setup shown in Fig. 5. The parameter range covered the wavelength range from 10 nm to 34 nm, the average pulse energy range of 20 μJ to 300 μJ and the pulse duration range of $\sim$ 50 fs to 300 fs FWHM. In this regime the experimentally measured pulse durations show no clear dependence on the fraction of the FEL beam used.

As pointed out in Ref. [12,19] the number of photoelectrons created in the interaction region has to be within a certain range to get a sufficiently strong signal but no undesired effects like space charge broadening. Thus, to ensure the same experimental conditions for all measurements, the streaking setup was left unchanged during the cutting mirror measurements, while the transmission of a variable XUV attenuator [19] was adapted such that the average number of created photoelectrons was constant for each cutting ratio. The gas attenuator is a 15-meter-long beam pipe filled with noble gases at a pressure of approximately 10^{-2} mbar. The interaction within the attenuator is linear, and no plasma formation occurs. Consequently, no changes in pulse duration are anticipated. To set up the measurement for a certain cutting fraction takes several minutes to half an hour. During this time the FEL parameters may drift and, thus, part of the observed pulse duration variations in Fig. 5 a) may be attributed to these drifts. In addition, it is to note that the error bars shown in Fig. 5 a) are not the measurement uncertainty but the rms width of the measured pulse duration distribution. We also verified that the XUV focal spot stays sufficiently smaller as compared to the THz focus for all cutting ratios.

Thus, we can reliably determine the *average* pulse duration in the measured parameter range by only using about 10 % of the FEL beam or even less. The evaluation shown in Fig. 5 a) considers only the pulse durations averaged over thousands of FEL pulses. To judge if the pulse duration for *single* FEL pulses, determined by measuring only a small fraction of the FEL beam,

Optics EXPRESS

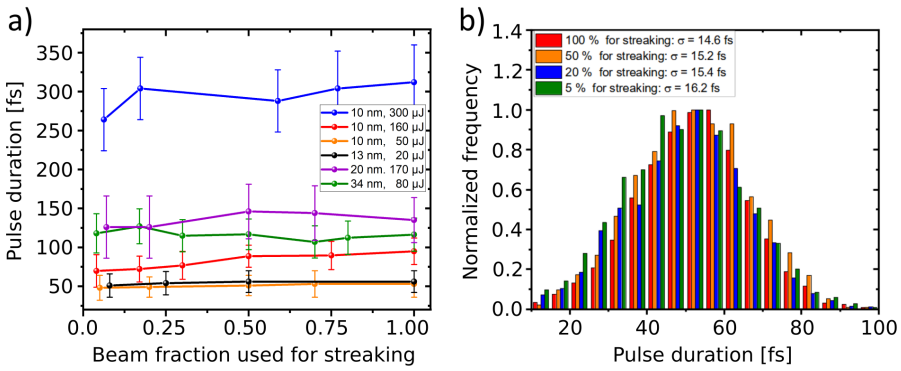

Fig. 5. Inserting the cutting mirror partially into the FEL beam (see Fig. 1) only part of the FEL beam is used for the pulse duration measurement. a) The plot shows the average pulse duration over few 1000 FEL pulses (points) and the rms width of the measured pulse duration distribution as error bars for various different FEL settings. We find no significant difference between the pulse duration determined with 10% of the FEL beam and larger fractions of the FEL beam. The observed small variations of the average pulse duration may also result from changes in the FEL during the lengthy measurement. b) The normalized pulse duration distributions of a few 1000 FEL pulses for several cutting ratio are shown. The histograms display pulse-resolved data from the 10 nm/ 50 fs (orange) measurement in plot a). Since the distribution is almost identical for the different cutting ratios, we infer that the pulse duration for a single FEL pulse measured on a fraction of the FEL beam resembles the pulse duration for the complete beam well. Part of the shown results were presented in [24]

is equivalent with the pulse duration of the complete beam is indeed much more challenging and can not be answered directly with the present setup. However, looking at the pulse duration distribution determined for different cutting ratios as displayed in Fig. 5 b), we do not see a large difference in the shape and width of the distributions. We interpret this as strong indication that also on a single shot basis the assumption that the pulse duration measured in only a fraction of the beam profile holds for the complete pulse is applicable. Here, clearly more experimental as well as simulation effort is needed to explore the approach in more detail and in particular for even shorter (few or single mode beams) FEL pulses.

4.2. Pulse duration measurements for users

Recently, we also started to support FLASH2 users on-demand with information about the FEL pulse temporal characteristics. Here we can provide the average pulse duration, the distribution of the XUV pulse duration and some information about a potential frequency chirp. Such a measurement could be carried out before and after a measurement campaign. Unfortunately, since FL21 has up to now no parasitic cutting mirror in the main beamline (see Fig. 1 a)), the measurement is not online and requires the switching of the entire XUV beam from the user beamline into FL21. Such a measurement usually takes about 2 hours. According to our experience during user beamtimes, when the FEL operates in a stable manner, there are only slight drifts in the pulse duration. It is planned to move the whole streaking setup upstream and incorporate the cutting mirror into the main beamline, such that the THz streaking measurements can be performed online with as little disturbance of the users as possible. A Python-based online analysis tool is developed that provides the temporal properties of the XUV pulses to operators (still in progress).

Optics EXPRESS

4.3. XUV arrival time measurements

The THz streaking setup is primarily designed to measure the XUV pulse duration. However, it can also determine the XUV arrival time with respect to the THz field. Since the IR laser producing the THz is well synchronized to FLASH MLO, we can compare the XUV arrival time to the electron bunch arrival time measured by the bunch arrival time monitor (BAM) [25], located in the acceleration section of the FEL.

For the THz streaking, the change of the mean photoelectron energy of the streaked pulse is proportional to the relative arrival time between the FEL XUV pulse and the THz slope [9,11,20]). The oscillator of the streaking laser is synchronized very well with a remaining jitter of only 5 − 10 fs rms via an optical cross correlator to FLASH MLO [20]. However, slow drifts by environmental changes (mainly temperature and air pressure) are accumulated during the amplification process. The regenerative amplifier [21] adds several tens of meters of path for the IR radiation during the amplification. This path is up to now not temporally stabilized (e.g. by a cross correlation between the amplified pulse and the oscillator) and thus slow temporal drifts of the amplified laser pulse in respect to the oscillator timing are present on a few minute scale. We corrected these slow drifts (± 30 fs) by using the drift stabilized BAM as reference and subtracting the difference between the two arrival time measurements from the streaking signal using a 5-min window averaging.

The electron bunch arrival time is measured by the BAM more than 200m upstream the FL21 endstation after the first accelerator modules at the location of the second bunch compressor (4DBC3) [20,25]. Here, the electron bunch arrival time is measured with an electro-optical method, utilizing directly the laser pulses from the drift-stabilized optical synchronization system, with a precision of typically 5 fs rms and no additional drifts are expected. The information about the electron arrival time is continuously measured for each FEL pulse and is available for user experiments. This data can be used to correct the arrival time during the data analysis and thus improve the temporal resolution of pump-probe experiments [26,27]. Our results emphasize that the arrival time measured by the BAM detectors is indeed extremely well correlated to the arrival time of the XUV photons, despite the large distance between BAM and experimental endstations. In addition, the arrival time information measured by the BAM can be used for a feedback acting on the accelerator to stabilize the electron bunch timing in respect to FLASH MLO [20,28].

Figure 6 presents BAM and THz streaking data from a long-term arrival time measurement for ~ 50000 FEL pulses acquired during ~ 80 minutes. The FEL was operating with 3 electron bunches spaced by 1 μs at a burst repetition rate of 10 Hz. The first bunch was streaked, while the two following pulses served as (unstreaked) reference. The electron bunches had a kinetic energy of 1.1 GeV and a bunch charge of 0.24 nC, resulting in XUV pulses at a wavelength of 10 nm (124 eV) and an average pulse energy of 160 μJ with an average pulse duration of ~ 100 fs (FWHM). The XUV photon (red dots) and electron (blue dots) arrival times are plotted on a shot-to-shot basis as well as 10 sec averaging using a second order Savitzky-Golay filter (red and blue lines) to illustrate the arrival time drifts. The first 60 minutes of the measurement were recorded with a "slow" arrival time feedback activated. Typically, an averaging window of 5 seconds is used in the slow feedback. Here, the arrival time fluctuation within the 60 min period was measured to be 24 fs rms by the BAM and 22 fs rms by the THz streaking. The slight difference may be attributed to the drift correction. For the last 20 minutes the feedback was switched off and one can see larger drifts of the arrival time yielding a larger widths of the arrival time distribution of 34 fs rms for BAM and 33 fs rms measured with the THz streaking. The corresponding histograms of the arrival times are plotted in Fig. 7 a) and d).

Comparing the two measurements by eye shows that the arrival time measured by streaking follows excellently the arrival time measured by the BAM. A comprehensive analysis of the arrival time data shows an rms deviation between the two methods of only 6 fs for the 10-second averaged data and a correlation width for the single shot analysis of 12-13 fs rms for the complete set of

Optics EXPRESS

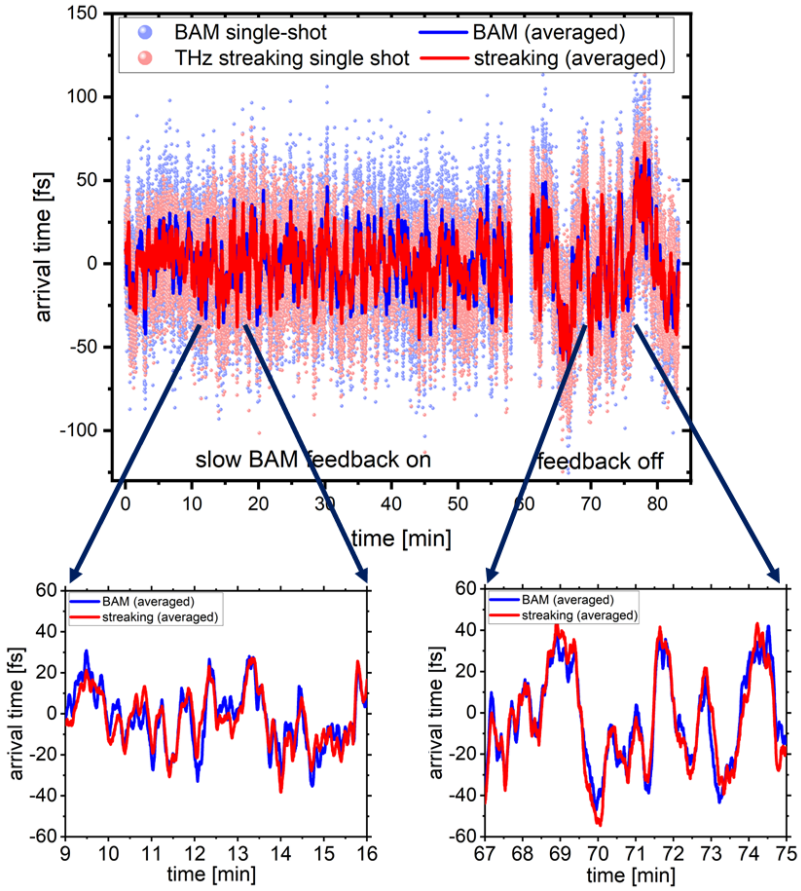

Fig. 6. Long-term measurement of the arrival time of ~ 50000 FEL pulses recorded by THz streaking and BAM. The single pulse arrival time is shown for the XUV photons (red dots) and the electron bunches (blue dots). The red and blue lines indicate a 10-second (100 pulses) averaging to illustrate the arrival time drifts. During the first 60 minutes of the measurement the "slow BAM feedback" is used to correct the arrival time of the accelerator, while for the last 20 minutes the feedback was switched off. The small figures at the bottom reveal in a zoomed view the good agreement of the 10 sec averaged measurement. More analysis is shown in Fig. 7.

data as shown in Fig. 7. This is most of all remarkable since there is a long list of possible jitter sources involved: Oscillator synchronization, THz streaking measurement uncertainty, BAM measurement uncertainty, SASE generation itself which leads to intrinsic timing fluctuations and possibly more unknown jitter sources. An elaborated explanation of measurement uncertainties using THz streaking can be found in [12]. Looking at the jitter budged in detail we can quantify the influence of some sources. For the BAM, the noise level of the measurement is continuously monitored and delivers ~ 5 fs rms measurement uncertainty. For the THz streaking, we have the uncertainty contribution of the synchronization of the laser oscillator with ~ 7 fs rms and the actual THz streaking measurement. Here, we have statistical fluctuations of the line shape (and thus fluctuations of the center of mass) by the limited number of electrons. This, one can estimate by comparing the difference in the arrival time measured by eTOF1 and eTOF2, resulting in an arrival time resolution of the streaking measurement of $5 - 10$ fs rms depending on the FEL settings. In addition FEL wavelength fluctuations and fitting errors account to about 4 fs rms.

Optics EXPRESS

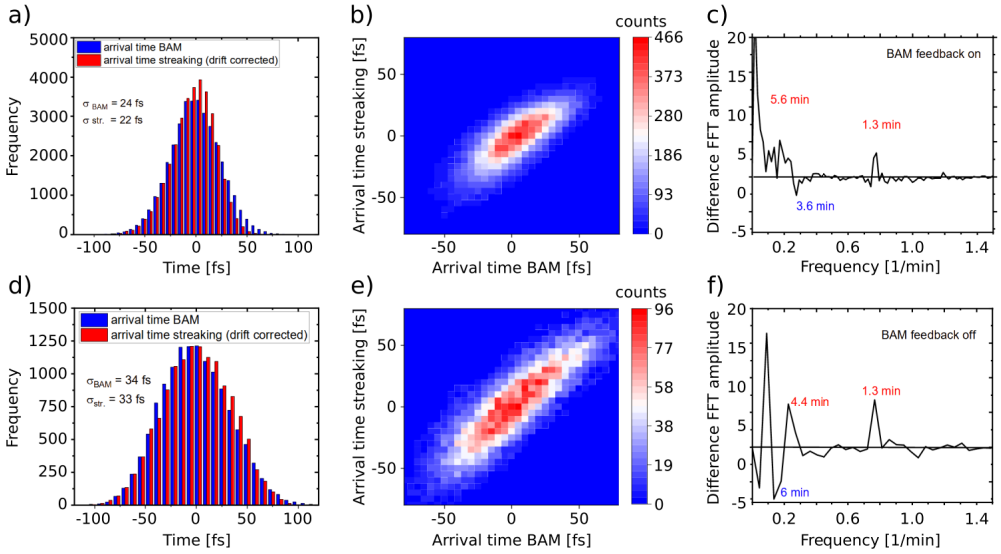

Fig. 7. Analysis of the arrival time data shown in Fig. 6. The upper row (a,b,c) shows the data with the arrival time feedback on, while the feedback was switched off for the lower row (d,e,f). a) and d) show the histograms of the arrival times measured with the BAM (blue) and the THz streaking(red). In addition the rms width of the histograms is displayed. b) and e) show the correlation plots of the arrival times measured with the BAM and THz streaking. The correlation width are only 12 fs rms for feedback on (b) and 13 fs rms (e) for feedback off. Finally, c) and f) present the difference of Fourier transformations (FFTs) of the arrival time data from BAM and THz Streaking (not drift corrected) indicating to individual sources causing the drifts. Positive peaks indicate deviations due to the THz streaking setup and negative are related to the BAM

Finally, the SASE induced arrival time fluctuations are predicted to be on the order of 4 fs rms for the given experimental FEL parameters following the equations in Ref. [13]. Adding up the known uncertainties quadratically according to the propagation of errors (since they result from independent sources) we end up at the measured 12-13 fs rms deviation between THz streaking and BAM, leaving little room for additional unknown jitter sources. Still, the knowledge of the various error sources limiting the arrival time measurements is of great importance to increase the time resolution for pump-probe experiments and will be further tackled by future measurement campaigns.

Besides the fast shot to shot jitter, slower arrival time drifts yield important information as well. To further investigate the temporal drifts, a fast Fourier transform (FFT) of the measurement results of both methods has been performed. Figure 7 c) and f) shows the difference of the FFTs. Thus, positive peaks indicate deviations caused by the THz streaking setup and negative are related to the BAM. Several distinct frequencies can be detected. The peak at 1.3 minutes in the THz streaking measurement can be referred to regulation cycles resulting from the chiller that stabilizes the temperature of the aluminum breadboard of the laser amplifier. What happens at the other peaks is still a subject of discussion. With this example, we want to show that our streaking setup can be used additionally for the characterization of different FEL diagnostics and subsystems.

Optics EXPRESS

5. Conclusion

FL21 at FLASH2, a new beamline for photon diagnostic developments, has been designed, built and commissioned. The beamline consists of two branches that can share the XUV radiation using a cutting mirror. With this mirror one can define the splitting ratio between the THz streaking branch and the straight section used as open port beamline including a focusing mirror. The FL21 THz streaking setup is a stand alone XUV pulse duration diagnostic setup with a dedicated optical laser system, THz generation and a photoelectron eTOF spectrometer chamber. This permanent setup allows long-term systematic studies of temporal properties of SASE radiation for various FEL settings. The well characterized installation also allows pulse duration measurements on rather short notice for user experiments. We showed that there is an excellent correlation between the arrival time measured by BAM (located 200 m upstream the experimental endstations) and the actual arrival time of the XUV photon pulse, highlighting that the BAM measurements can be used to enhance the temporal resolution for user pump-probe experiments. Pulse duration measurements using different fractions of the FEL pulse for the measurement show, that the concept to use a "cutting mirror" allows a virtually parasitic online diagnostic in future. The experimental results support the assumption that the pulse duration measured from a small part of the FEL beam holds for the complete pulse.

In general, a permanently installed, well characterized and easy-to-use pulse duration setup can be used efficiently to determine SASE properties (like the pulse duration along the undulator [19] or Chirp), 2-color operation [29], pulse duration of FEL harmonics, or moreover use the setup to investigate atomic physics e.g. [30,31].

Acknowledgments. We want to acknowledge Anne-Laure Calendron, Joachim Meier, and Simon Reuter (DESY, XFEL) for their support and help regarding the regenerative amplifier. We also want to thank the DESY Synchronization group (in particular Sebastian Schulz) for providing an excellent synchronization of our laser. We would like to acknowledge Kai Tiedke (DESY) for useful discussions and suggestions for improving this article. In addition we acknowledge the help of Luca Poletto and Paolo Miotti (CNR-IFN) for their support in designing the XUV beamline optics. We also thank the FLASH operators for helpful discussions and for fulfilling our special wishes during our beamtimes.

Disclosures. The authors declare no conflicts of interest.

Data Availability. The data presented in this study are available on request from the corresponding authors.

References

1. W. Ackermann, G. Asova, and V. Ayvazyan, *et al.*, "Operation of a free-electron laser from the extreme ultraviolet to the water window," Nat. Photonics **1**(6), 336–342 (2007).
2. P. Emma, R. Akre, and J. Arthur, *et al.*, "First lasing and operation of an ångstrom-wavelength free-electron laser," Nat. Photonics **4**(9), 641–647 (2010).
3. T. Ishikawa, H. Aoyagi, and T. Asaka, *et al.*, "A compact X-ray free-electron laser emitting in the sub-ångström region," Nat. Photonics **6**(8), 540–544 (2012).
4. W. Decking, S. Abeghyan, and P. Abramian, *et al.*, "A MHz-repetition-rate hard X-ray free-electron laser driven by a superconducting linear accelerator," Nat. Photonics **14**(6), 391–397 (2020).
5. C. J. Milne, T. Schietinger, and M. Aiba, *et al.*, "Swissfel: The swiss x-ray free electron laser," Appl. Sci. **7**(7), 720 (2017).
6. I. S. Ko, H.-S. Kang, and H. Heo, *et al.*, "Construction and Commissioning of PAL-XFEL Facility," Appl. Sci. **7**(5), 479 (2017).
7. S. Düsterer, M. Rehders, and A. Al-Shemmary, *et al.*, "Development of experimental techniques for the characterization of ultrashort photon pulses of extreme ultraviolet free-electron lasers," Phys. Rev. Spec. Top.–Accel. Beams **17**(12), 120702 (2014).
8. U. Frühling, M. Wieland, M. Gensch, T. Gebert, B. Schütte, M. Krikunova, R. Kalms, F. Budzyn, O. Grimm, J. Rossbach, E. Plönjes, and M. Drescher, "Single-shot terahertz-field-driven X-ray streak camera," Nat. Photonics **3**(9), 523–528 (2009).
9. I. Grguraš, A. R. Maier, C. Behrens, T. Mazza, T. J. Kelly, P. Radcliffe, S. Düsterer, A. K. Kazansky, N. M. Kabachnik, Th. Tschentscher, J. T. Costello, M. Meyer, M. C. Hoffmann, H. Schlarb, and A. L. Cavalieri, "Ultrafast X-ray pulse characterization at free-electron lasers," Nat. Photonics **6**(12), 852–857 (2012).
10. P. L. Kramer, M. K. R. Windeler, M. K. R. Windeler, K. Mecseki, E. G. Champenois, M. C. Hoffmann, and F. Tavella, "Enabling high repetition rate nonlinear THz science with a kilowatt-class sub-100 fs laser source," Opt. Express **28**(11), 16951–16967 (2020).

Optics EXPRESS

11. R. Ivanov, J. Liu, G. Brenner, M. Brachmanski, and S. Düsterer, "FLASH free-electron laser single-shot temporal diagnostic: terahertz-field-driven streaking," J. Synchrotron Radiat. **25**(1), 26–31 (2018).
12. R. Ivanov, I. J. B. Macias, J. Liu, G. Brenner, J. Roensch-Schulenburg, G. Kurdi, U. Frühling, K. Wenig, S. Walther, A. Dimitriou, M. Drescher, I. P. Sazhina, A. K. Kazansky, N. M. Kabachnik, and S. Düsterer, "Single-shot temporal characterization of XUV pulses with duration from ~10 fs to ~350 fs at FLASH," J. Phys. B: At., Mol. Opt. Phys. **53**(18), 184004 (2020).
13. I. J. B. Macias, S. Düsterer, R. Ivanov, J. Liu, G. Brenner, J. Rönsch-Schulenburg, M. K. Czwalinna, and M. V. Yurkov, "Study of temporal, spectral, arrival time and energy fluctuations of sase fel pulses," Opt. Express **29**(7), 10491–10508 (2021).
14. F. Sorgenfrei, W. F. Schlotter, T. Beeck, M. Nagasono, S. Gieschen, H. Meyer, A. Föhlisch, M. Beye, and W. Wurth, "The extreme ultraviolet split and femtosecond delay unit at the plane grating monochromator beamline PG2 at FLASH," Rev. Sci. Instrum. **81**(4), 043107 (2010).
15. M. Sauppe, D. Rompotis, and B. Erk, *et al.*, "XUV double-pulses with femtosecond to 650ps separation from a multilayer-mirror-based split-and-delay unit at FLASH," J. Synchrotron Radiat. **25**(5), 1517–1528 (2018).
16. M. Wöstmann, R. Mitzner, T. Noll, S. Roling, B. Siemer, F. Siewert, S. Eppenhoff, F. Wahlert, and H. Zacharias, "The XUV split-and-delay unit at beamline BL2 at FLASH," J. Phys. B: At., Mol. Opt. Phys. **46**(16), 164005 (2013).
17. M. Dreimann, F. Wahlert, D. Eckermann, F. Rosenthal, S. Roling, T. Reiker, M. Kuhlmann, S. Toleikis, M. Brachmanski, R. Treusch, E. Plönjes, B. Siemer, and H. Zacharias, "The soft X-ray and XUV split-and-delay unit at beamlines FL23/24 at FLASH2," J. Synchrotron Radiat. **30**(2), 479–489 (2023).
18. A. A. Sorokin, A. Gottwald, A. Hoehl, U. Kroth, H. Schöppe, G. Ulm, M. Richter, S. V. Bobashev, I. V. Domracheva, D. N. Smirnov, K. Tiedtke, S. Düsterer, J. Feldhaus, U. Hahn, U. Jastrow, M. Kuhlmann, T. Nunez, E. Plönjes, and R. Treusch, "Method based on atomic photoionization for spot-size measurement on focused soft x-ray free-electron laser beams," Appl. Phys. Lett. **89**(22), 221114 (2006).
19. M. M. Bidhendi, I. J. Bermudez Macias, R. Ivanov, M. V. Yurkov, and S. Düsterer, "Fel pulse duration evolution along undulators at flash," Appl. Sci. **12**(14), 7048 (2022).
20. S. Schulz, I. Grguraš, C. Behrens, H. Bromberger, J. T. Costello, M. K. Czwalinna, M. Felber, M. C. Hoffmann, M. Ilchen, H. Y. Liu, T. Mazza, M. Meyer, S. Pfeiffer, P. Prędki, S. Schefer, C. Schmidt, U. Wegner, H. Schlarb, and A. L. Cavalieri, "Femtosecond all-optical synchronization of an X-ray free-electron laser," Nat. Commun. **6**(1), 5938 (2015).
21. A.-L. Calendron, H. Çankaya, and F. X. Kärtner, "High-energy khz yb:kyw dual-crystal regenerative amplifier," Opt. Express **22**(20), 24752–24762 (2014).
22. J. Hebling, G. Almási, I. Z. Kozma, and J. Kuhl, "Velocity matching by pulse front tilting for large-area thz-pulse generation," Opt. Express **10**(21), 1161–1166 (2002).
23. U. Frühling, "Light-field streaking for FELs," J. Phys. B: At., Mol. Opt. Phys. **44**(24), 243001 (2011).
24. I. J. Bermudez Macias, "Free electron laser pulse characterization by THz streaking," Doctoral dissertation, University of Hamburg, (2022).
25. A. Angelovski, M. Kuntzsch, M. K. Czwalinna, A. Penirschke, M. Hansli, C. Sydlo, V. Arsov, S. Hunziker, H. Schlarb, M. Gensch, V. Schlott, T. Weiland, and R. Jakoby, "Evaluation of the cone-shaped pickup performance for low charge sub-10 fs arrival-time measurements at free electron laser facilities," Phys. Rev. Spec. Top.–Accel. Beams **18**(1), 012801 (2015).
26. D. Mayer, F. Lever, and M. Gühr, "Data analysis procedures for time-resolved x-ray photoelectron spectroscopy at a SASE free-electron-laser," J. Phys. B: At., Mol. Opt. Phys. **55**(5), 054002 (2022).
27. E. Savelyev, R. Boll, and C. Bomme, *et al.*, "Jitter-correction for IR/UV-XUV pump-probe experiments at the FLASH free-electron laser," New J. Phys. **19**(4), 043009 (2017).
28. B. Lautenschlager, L. Butkowski, M. Czwalinna, B. Dursun, M. Hierholzer, S. Pfeiffer, H. Schlarb, and C. Schmidt, *Arrival Time Stabilization at Flash Using the Bunch Arrival Corrector Cavity (BACCA)* (JACOW Publishing, Geneva, Switzerland, 2021).
29. E. Schneidmiller, I. J. Bermudez Macias, M. Beye, M. Braune, M. K. Czwalinna, S. Düsterer, B. Faatz, R. Ivanov, U. F. Jastrow, M. Kuhlmann, J. Rönsch-Schulenburg, S. Schreiber, A. Sorokin, K. Tiedtke, M. Yurkov, and J. Zemella, "Two-Color Operation of a Soft X-ray FEL with Alternation of Undulator Tunes," Appl. Sci. **13**(1), 67 (2022).
30. I. J. B. Macias, S. Düsterer, R. Ivanov, U. Frühling, and N. M. Kabachnik, "Post-collision interaction effect in THz-assisted Auger decay of noble gas atoms," J. Phys. B: At., Mol. Opt. Phys. **54**(8), 085601 (2021).
31. I. J. B. Macias, I. P. Sazhina, R. Ivanov, S. Düsterer, and N. M. Kabachnik, "Time-dependent post-collision-interaction effects in THz-field-assisted Auger decay," Phys. Rev. A **104**(5), 053102 (2021).